International Journal of Sustainable and Green Energy
2021; 10(4): 108-120
http://www.sciencepublishinggroup.com/j/ijsge
doi: 10.11648/j.ijrse.20211004.11
ISSN: 2575-2189 (Print); ISSN: 2575-1549 (Online)

Analytical Behaviour of BPS150-36 Polycrystalline Modules Electrical Parameters with Ambient Temperature Under Standard Conditions Using Servant Model

Hounkpatin Florentin Géraud, Madogni Vianou Irénée*, Agbomahéna Bienvenu Macaire, Kounouhéwa Bruno Basile

Département de Physique (FAST/LPR), Université d'Abomey-Calavi (UAC), Abomey-Calavi, Bénin

Email address:
madognimadogni@gmail.com (M. V. Irénée)
*Corresponding author

To cite this article:
Hounkpatin Florentin Géraud, Madogni Vianou Irénée, Agbomahéna Bienvenu Macaire, Kounouhéwa Bruno Basile. Analytical Behaviour of BPS150-36 Polycrystalline Modules Electrical Parameters with Ambient Temperature Under Standard Conditions Using Servant Model. *International Journal of Sustainable and Green Energy*. Vol. 10, No. 4, 2021, pp. 108-120. doi: 10.11648/j.ijrse.20211004.11

Received: June 20, 2019; **Accepted**: July 23, 2019; **Published**: October 21, 2021

Abstract: (PV)-cells/modules demonstrated low performance in hot-humid climates because elevated ambient temperature conditions significantly influence their performance. We investigated analytically the behaviour of BPS150-36 polycrystalline silicon (PV)-modules electrical parameters with ambient temperature under standard irradiation conditions (STC), using Servant model. Matlab and r.getdata have been used for the numerical simulations. Results obtained show that (J_{Ph}) increases exponentially from 7.67% to 65.87% with temperature. (R_S) increases linearly by 7.6% and 9.18% while (V_{OC}) decreases from 19.4 % to 17.6% and (R_{Sh}) decreases approximately by 12.6% and 4.8%. The obtained power output (P) losses had been 82.31 % and 31.56%, and the overall linear losses in efficiency (η) had been approximately 27.84% and 5.02 %, while (J_S) increases exponentially from 3.87% to 15.75%. The increase in (J_{Ph}) with temperature can be attributed to the increased in light absorption owing to a decrease in the bandgap of silicon. The decrease in (η) with temperature is mainly controlled by the decrease in (V_{OC}) and fill factor (FF) with T. Power output loss is strongly attributed to the decrease of the fill factor (FF) due to an increase in series resistance (R_S) and therefore caused by the (J_{SC}) degradation.

Keywords: Low Performance, Behaviour, Standard Irradiation Condition, Servant Model, Increase, Decrease, Degradation

1. Introduction

Several studies have been presented in the literature summarizing, the different modes of failures that are commonly observed for (PV)-modules in various regions (desert, arid, and tropical zones) [1-3]. Many early degradation mechanisms (light-induced degradation of solar cells, discoloration, and delamination of encapsulant materials) have been studied [4-6]. The long-time degradation and defects generated in field aged PV modules (solar cell corrosion and solder ribbon, crack in solder joint and cell breakage) have been considered to be common causes of the (PV)-modules failures [7-9]. Therefore, (PV)-cells/modules performances and ageing strongly depend on the climate and the environment of the installation site. Indeed, the performances of (PV)-cells/modules under real conditions depend on the weather, the solar spectrum, the spectral response of each technology, and the module/cell design [10-13]. (PV)-cells/modules performance is characterized by a number of electrical parameters: short circuit current density (J_{SC}), open circuit voltage (V_{OC}), fill factor (FF), and efficiency (η) [14]. The overall performance of a PV cell is represented by (η), which depends on the other three performance parameters: (J_{SC}), (FF) and (V_{OC}) [15]. The value of (J_{SC}) increases with P_{in}, but does not significantly affect (η) because this increase is linear (J_{SC} is linearly dependent on (P_{in})). By increasing the solar radiation, (V_{OC}) increases logarithmically whereas the (J_{SC}) elevates linearly, as an upshot the resulting power increase [14-16]. As the cell temperature increases the efficiency drops by lowering the (V_{OC}) and a slight decrease of (J_{SC}). The effects of various parameters on the solar cell functioning have been summarized in Table 1 [16-20].

Table 1. *Summary of various influential parameters on PV cells/modules performance.*

Parameters	dependency	Influential factor
Cell photocurrent (J_{ph})	Depend on	Irradiance and wavelength
(V_{OC})	Logarithmically dependent on	Illumination
(J_{SC})	Dependent on	Illumination
Fill factor (FF)	Increases by	Series resistance decrease
Fill factor (FF)	Increases by	Shunt resistance increase
(V_{OC})	Decreases by	Temperature rise
(J_{SC})	Nearly constant by	Temperature rise
Fill factor (FF)	Decreases by	Temperature rise

The correlation of the visual defects and the shifts in the electrical parameters has been analyzed [21], and the different failure mode, failure causes and failure mechanisms of (PV)-module for different climatic conditions have been investigated [22]. The average peak power decay/year in composite climate has been found to be 14.6% in a-Si array modules, 1.7% in poly-C-Si array modules and 1.5% in the HIT (hetero-junction intrinsic thin layer) array modules respectively, which corresponds to loss in either short circuit current (Isc) or fill factor (FF) or both [23]. After thirty (30) years of experimentation, it has been reported that the average peak power degradation of crystalline silicon PV modules have been found to be 13.86% of initial value for the modules installed in Libya [24, 25]. Moreover, the degradation of 731 SM55 monocrystalline silicon photovoltaic modules has been analyzed. After eighteen (18) Years of operation in hot-humid climatic conditions, the median maximum power (P_m), open-circuit voltage (V_{oc}), short-circuit current (I_{sc}) and fill factor (FF) decreased by 24.38%, 2.02%, 7.37%, and 15.74%, respectively, as compared with the nameplate values. More detailed set of data regarding the degradation of electrical parameters is given in Table 2 [26]. It appears that the annual degradation of the power output of the modules varies between 0.94% per year and 2.51% per year, with a median value of 1.54% per year [25, 26]. These values of degradation are significantly higher than what is usually assumed for mono-crystalline silicon PV modules. The reduction of power output is mainly attributed to the decrease of the fill factor (FF). The degradation of the fill factor (FF) has been found to be due to an increase in series resistance (R_S) of the modules caused by solder bond failure and the corrosion of the Ag electrodes [26].

Table 2. *Values of the Minimum, Maximum, Average, Median, and Standard deviation degradation of the power output, open-circuit voltage, short-circuit current, and fill factor of the PV modules after eighteen (18) years exposure [26].*

Parameters	Minimum Degradation	Average Degradation	Median Degradation	Maximum Degradation	Standard Deviation
Power Output (P_m)	15,61%	24,62%	24,38%	36,76%	3,89%
Open-circuit voltage (V_{oc})	0,70%	2,40%	2,02%	3,35%	0,46%
Short-circuit current (I_{sc})	1,79%	7,72%	7,37%	15,78%	1,85%
Fill factor (FF)	5,45%	16,25%	15,74%	32,84%	4,41%

In another similar study [27], the performance of 40 crystalline silicon (mono and multi) PV modules after 20-22 years field exposure has been analyzed. They revealed that modules encapsulated with EVA and a Tedlar aluminum back sheet exhibited 14.8% mean power degradation while module with encapsulated silicon sealant showed average power degradation of 6.4%. Likewise, [28] obtained 0.5%/year power degradation in c-Si (PV)-modules after ten (10) years outdoor exposure. They concluded that this rate obtained was due to the delamination between cell and EVA, and metallization of solder bond.

Recently, the performance degradation of mono-C-Si in Indian climate after twelve (12) years of outdoor exposure for the modules manufactured by eleven (11) different Indian manufactures has been investigated [29]. The rate of output power degradation has been evaluated between 5-16.5% for the modules whose module qualified under IEC 61215 standards after ten (10) years. But, seventeen (17) and 33% output power degradation has been obtained for the modules that are not qualified under IEC 61215 standards after ten (10) years out-door exposure [29]. Likewise, the 11.5% peak power degradation obtained by [30] were totally due to the short circuit current (I_{SC}). After twenty-eight (28) years outdoor exposure of the mono-C-Si PV modules, [31] reported that 1.4%/year average power degradation for PV generator. It was due to encapsulate discoloration, delamination and oxidation of front grid finger, anti-reflecting coating and bubbles in back-sheet. [32] showed that after few years operation of c-Si PV module in tropical climate Dakar, Senegal, the highest loss in the maximum power output has been evaluated of 0.22%/year to 2.96%/year. But, the open-circuit voltage has not been degraded. Oxidation of the anti-reflective coating, cell metallization grid, glass weathering and delamination at the cell-EVA interface have been found to be most frequently occurring defects [4-9, 31, 32].

According to [25], the effects of degradation over period of twenty-two (22) years on the parameters I_{SC}, V_{OC}, FF and Power indicated that I_{SC} degraded from 0.4% to 3.7% with an average value 1.8%/year. The average value of V_{OC} degradation rate is 1.4%/year and FF ranges from 0.7% to 2.6% with an average value of 1%/year. The power degradation rate ranges from 0.3% to 4.1% with an average value of 1.9%/year. The degradation in power output is mainly due to the degradation in the I_{SC} [25, 26, 32].

Through these different investigations aforementioned, there is not yet a complete understanding of what qualification test or test sequence is required to guarantee that a particular PV module would survive twenty-five (25) years in a particular climate. As you know, the degradation rate or the lifetime of (PV)-modules and systems are greatly influenced by the climatic conditions [33], but the exact

understanding of the influence of temperature, thermal cycling, UV exposure, relative humidity, or a combination of these is far from being established [34].

This theoretical approach adds more data to the (PV)-module degradation study in tropical climate. Our aim is to analyze how the electrical parameters are degraded during the cells/modules operating conditions in order to proceed to a statistical investigation of these parameters degraded under standard irradiation conditions (STC) (G=1000W/m^2) in the 298-348K temperature range, using the Servant model [35]. As you know that, one of the main factors influencing the (PV)-cells/modules temperature is ambient temperature, but there is a linear relationship between (PV)-module temperature and ambient temperature. However, the module temperature strongly depends on many parameters such as solar radiation, ambient temperature, wind speed, air humidity, speed and direction of the wind, PV module orientation, dust and sand deposition on PV module, PV module materials used, and other meteorological parameters [35, 36]. Consequently, the ambient temperature is one of the most important factors that affect the global (PV)-cells/modules performance.

The rest of this paper is structured as follows. Theory and modeling have been presented and established in Section 2. Next, the results are analyzed and discussed in section 3. Finally, the conclusions and outlooks end the paper in section 4.

2. Materials and Methods

2.1. Electrical Operating Conditions

Temperature is a very important parameter in functioning of PV cells because cells electrical properties are sensitive to temperature [37]. But heat stress causes cracking and burning of cells, and reduces the current produced by the module. Most of the electrical parameters of PV modules depend on the temperature and the solar irradiation. Once all these parameters are determined within reference conditions, their new values can be determined in any real operating conditions [38-44], using the following models represented by the Equations (1)-(14) below.

2.1.1. Photocurrent Density (J_{ph})

In most of the studies, the photocurrent density (J_{ph}) is approximated by the short circuit current density [40, 45, 46]. This assumption is generally accepted for the modeling of (PV)-module or cell because in real devices the series resistance is low while the parallel resistance is high. This parameter is often considered as a good starting point in several defined iterative algorithms [41].

$$J_{ph}(G,T) = J_{ph_{ref}}\left[1 + \alpha_{J_{SC}}\left(T_m - T_{ref}\right)\right]\frac{G}{G_{ref}} \quad (1)$$

where T_{ref}: Solar cell temperature in reference condition, G_{ref}: Solar irradiation in reference condition, G: Solar irradiation, T_m: Module temperature, $\alpha_{J_{SC}}$: Temperature coefficient of the short-circuit current density, $J_{ph_{ref}}$: Short-circuit current density in reference conditions.

2.1.2. Saturation Current Density (J_S)

The rates of the saturation current density change with the cell temperature according to Equations (2) and (3) for one-diode [40] and two-diode model [41, 47] respectively. Authors report that the equations are suitable for all technology of silicon solar cells [40, 41, 47].

$$J_S = J_{S_{ref}} \times \left(\frac{T_m}{T_{ref}}\right)^3 \times exp\left(\frac{1}{K}\left(\frac{E_{g_{ref}}}{T_{ref}} - \frac{E_g(T_m)}{T_m}\right)\right) \quad (2)$$

with $\frac{E_g(T)}{E_{g_{ref}}} = 1 - 0.0002677\ (T_m - \mathrm{T_{ref}})$

and

$$J_{S_i} = J_{S_{ref}} \times \left(\frac{T_m}{T_{ref}}\right)^{\frac{3}{ni}} \times exp\left(\left(\frac{E_g(T)}{ni.K}\right)\left(\frac{1}{T_{ref}} - \frac{1}{T_m}\right)\right) \quad (3)$$

with $i = 1, 2$ and $E_g(T) = 1.17 - 0.000673 \times \frac{T_m^2}{T_m + 636}$

where: $J_{S_{ref}}, J_S$ the saturation current density in reference and real conditions respectively, K: Boltzmann constant (J.K^{-1}) and $E_g(T)$: Bandgap energy [40].

2.1.3. Series (R_S) and Shunt (R_{Sh}) Resistance

The series resistance ($\mathrm{R_S}$) of a PV module arises from resistances in cell solder bonds, cell metallization, cell-interconnect bus-bars and resistances in junction-box terminations [47, 48]. This resistance exhibits a variation given by the temperature coefficient for the ambient temperature, approximately expresses how the specific value varies according to a rise in temperature value.

$$R_j = R_{ref}\left[1 + a\left(j - T_{ref}\right)\right] \quad (4)$$

where R_j: Résistance at a given temperature (Ω): R_{ref}: Series resistance in the reference conditions, a: Temperature coefficient (1/k) and j: given temperature (°C). The series resistance increases proportionally with the elevation of temperature. This increase in series resistance causes a decrease in the voltage, and therefore power [49]. In addition, the decrease in shunt resistance ($\mathrm{R_{Sh}}$) is to increase the leakage current around the cells, because the increase in temperature will liberate charge carriers, which in turn brings down the maximum power. It seems that the right way to determine (R_S) and (R_{Sh}) should take into account the thermal parameters of the material. Nevertheless, the following methods [38-40] give good results for the two types of model.

$$R_S = \frac{R_{S_{ref}} \times T_m}{T_{ref}}\left(1 - \beta \times ln\frac{G}{G_{ref}}\right) \quad (5)$$

where β, is a coefficient which value is approximately 0.217 and $R_{S_{ref}}$: Series resistance in reference conditions.

$$R_{Sh} = R_{Sh_{ref}} - m_o \times T_m \quad (6)$$

$R_{ph_{ref}}$: Shunt resistance in reference conditions and m_o: is a coefficient which value is approximately $6.8936\ \Omega Cm^2/K$ [3].

2.1.4. Open-circuit Voltage (V_{OC})

The main temperature dependence in (PV)-cells/modules arises from variation of three main parameters, which are usually used to characterize the solar cell outputs, these are: (J_{SC}), the short-circuit current density, which usually has a negative sign, the open-circuit voltage (V_{OC}) which is characterized by (J_S), the diode saturation current, and n, the diode ideality factor, and the fill factor (FF), which in turn is a function of (V_{OC}). (V_{OC}) is given as follows [50]:

$$V_{OC} = \frac{n\,k\,T_m}{q} \ln\left[1 - \frac{G_{Sh}V_{OC}}{J_S} + \frac{J_{ph}}{J_S}\right] \quad (7)$$

For $J_{ph} \gg G_{Sh}V_{OC}$ and $J_{ph} \gg J_S$, a linear dependence between V_{OC} and Tm has been established.

$$V_{OC} = \frac{E_g}{q} - \frac{n\,k\,T_m}{q} \times \ln\left(\frac{J_S}{J_{ph}}\right) \quad (8)$$

E_g: Bandgap energy.

2.1.5. PV Module Efficiency Models

(PV)-cell/module performance is influenced by temperature as its performance parameters: open-circuit voltage (V_{OC}), short-circuit current density (J_{SC}), fill factor (FF) and efficiency (η) are temperature dependent. It has been shown earlier that (V_{OC}) decreases at a rate of 2.3 mV/K whereas (J_{SC}) increases slightly with module temperature (T_m). (FF) also decreases and all these lead to an overall decrease in the cell efficiency (η) [51].

It turns out that both open circuit voltage (V_{OC}) and fill factor (FF) decrease substantially with temperature, while short-circuit current (J_{SC}) increases, but only slightly [51, 52]. All these effects lead to a linear relation in the form:

$$\eta = \eta_{T_{ref}}\left[1 - \beta_{ref}\left(T_m - T_{ref}\right) + \gamma\, log_{10}G_T\right] \quad (9)$$

$\eta_{T_{ref}}$: Module electrical efficiency at the reference temperature, T_m: PV module temperature, T_{ref}: Reference temperature at solar radiation flux of 1000W/m^2,

$\beta_{ref} = \frac{1}{T_O + T_{ref}}$: Temperature coefficient, γ: Solar radiation coefficient and T_O: the high temperature at which the PV module's electrical efficiency drops to zero [51, 53, 54].

A reduced expression of the model has been proposed by [55], neglecting the solar radiation coefficient:

$$\eta = \eta_{T_{ref}}\left[1 - \beta_{ref}\left(T_m - T_{ref}\right)\right] \quad (10)$$

In these analytical models, the cell/module temperature which is not readily available has been replaced by the nominal operating cell temperature (T_{NOCT}) and we have [56]:

$$\eta = \eta_{ref}\left\{1 - \beta_{ref}\left[T_{amb} - T_{ref} + (T_{NOCT} - T_{amb})\frac{G_T}{G_{NOCT}}\right]\right\} \quad (11)$$

In which

$$T_{amb} = T_m - \left(\frac{G_T}{G_{NOCT}}\right)\left(\frac{U_{L,NOCT}}{U_L}\right)\left(T_{NOCT} - T_{amb,NOCT}\right)\left[1 - \left(\frac{\eta_c}{\tau\alpha}\right)\right] \quad (12)$$

An analytical model of the monthly average efficiency has been proposed by [57], in order to estimated the monthly electrical energy output of a PV array.

$$\bar{\eta} = \eta_{Tref}\left[-1 - \beta_{ref}\left(\overline{T}_{amb} - T_{ref}\right) - \frac{\beta_{ref}(\overline{\tau\alpha})\overline{H}_T\overline{V}}{nU_L}\right] \quad (13)$$

where, n: Number of hours per day, U_L: overall thermal loss coefficient, $\overline{H}_T$: the monthly average daily insolation on the plane of the array, $\overline{V}$: a dimensionless function of such quantities as the sunset angle.

2.1.6. PV Module Power Output Models

(PV)-cell/module performance prediction in terms of electrical power output in the field, that is, the deviation from the standard test conditions reported by the manufacturer of the module, is analytically modeled in a manner analogous to the module efficiency. Recently, [58] proposed a correlation for PV module power, similar in form to Equation 10.

$$P = G_T\tau_{pV}\eta_{ref}\,A\left[1 - \beta_{ref}\left(T_m - T_{ref}\right)\right] \quad (14)$$

τ_{pV}; Transmittance of the PV cell outside layers.

2.2. Servant Model

Direct exposure of (PV)-module surface to the solar radiation causes the (PV)-module operating conditions more sensitive to the module temperature. So, temperature as an important factor that affects the module efficiency and the generated electric power of (PV)-modules. Then temperature is one of the most important parameters for assessing the long-term performance and the output energy of (PV)-module. The module temperature increases lead to a decrease in the output voltage. Moreover, the temperature increases lead to a slight increase in the output current that can be ignored in the output module power. Then the increased temperature makes degradation in the module output power [36].

Servant model is based on the heat exchange between the PV module and the atmosphere. It allows obtaining the module temperature according to ambient temperature (T_{amb}), and meteorological parameters [35, 36].

$$T_m = T_{amb} + d \times G \times (1 + e \times T_{amb})(1 - f \times W) \quad (15)$$

where W: wind speed, d, e and f: Parameters that are calculated empirically, and T_{amb}: ambient temperature.

3. Results and Discussions

3.1. Cells/Modules Characteristics (Data Sheet)

We used BPS150-36 polycrystalline silicon cells (156mm×156mm), connected in series with a maximum power 150 Watts.

(1) Maximum supply voltage: 18V; Maximum power current: 8.33A;
(2) Open circuit-voltage: 21.60 V; Current short-circuit current: 9.08A;
(3) Battery performance: 16.5%; Cells number (Pcs): 36;
(4) Size of portable: 156*156mm;
(5) Module size: 1480*680*35mm;
(6) Maximum system voltage: 1000 V;
(7) Fill factor (FF) ≥ 72% ;
(8) Frame (material, corners, etc.) aluminum; Output tolerance: ±5% ;
(9) Cable length: 900mm; junction box type: PKJB001 (TUV);
(10) Weight per piece: 13 kg; Connectors and cables type: with TUV certificate;
(11) Maximum surface load capacity: 60 m/s (200 kg/m^2).

i Relative coefficients to the temperature:
(1) Temperature coefficient of J_{SC} (%): + 0,1/°C;
(2) Temperature coefficient of V_{OC} (%): −0.38/°C;
(3) Temperature coefficient of PM (%): −0.47/°C;
(4) Temperature coefficient of JM (%): −0.1/°C;
(5) Temperature coefficient of VM (%): −0.38/°C;
(6) Temperature range: from -40°C to +85°C.

(J-V) characteristics of modules have been measured under STC with solar radiation: 1000W/m^2, spectrum: AM1.5G, module temperature: 25°C.

ii Analytical characteristics

The structure of polycrystalline silicon module is modeled by the equivalent electrical circuit (figure 1) with a single diode [11].

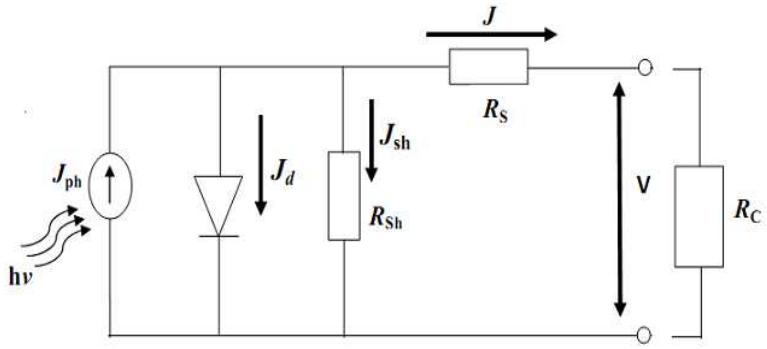

Figure 1. *Equivalent electrical circuit of polycrystalline silicon photovoltaic module under an incident illumination.*

According to the nodes and meshes laws, we have:

$$J + J_{ph} = J_d + J_{Sh} \text{ and } V = JR_S + J_{Sh} \times R_{Sh} \quad (16)$$

Using the expression for the current-voltage characteristic of PV, we find the expression for J as:

$$J = J_{ph} - J_S\left[exp\left(\frac{q(V + R_S J)}{nK_B T}\right) - 1\right] - \frac{(V + R_S J)}{R_{Sh}} \quad (17)$$

Therefore, the transcendental analytic equation for the optimal current J_{opt} of the ideal PV module is described by [59]:

$$J_{opt} = \frac{J_{Ph} + J_S}{1 + \frac{1}{\ln\left(\frac{J_{Ph} - J}{J_S}\right) + 1}} \quad (18)$$

With

$$V_{opt} = \frac{k\ T_m}{q} \ln\left(\frac{J_{Ph} - J}{J_S} + 1\right) \quad (19)$$

where $J_{Ph}\,(A/cm^2)$: Photo-induced current-density determined by the spectral composition, intensity, and concentration of incident solar radiation and also by the efficiency of assembling photogenerated p-n junction charge carriers, $J_S(A/cm^2)$: the reverse dark photoinduced saturation current-density determined by potential and electro-physical parameters of p-n junction, T_m (°K): PV module temperature, k: the Boltzmann constant; and q(C) is the electron charge.

When the PV module is illuminated by solar light $J_{Ph} \gg J_S, J_{Ph} - J \gg J_S$, the logarithm in the denominator of J_{opt} is a higher value and does not vary much with variations in J. Then, the transcendental equation is solved by stepwise approximations. For $J = 0$, we have:

$$J_{opt} = \frac{J_{Ph}}{1 + \frac{1}{\ln\left(\frac{J_{Ph}}{J_S}\right)}} \quad (20)$$

and the optimal voltage becomes:

$$V_{opt} = \frac{k\ T_m}{q}\left[\ln\left(\frac{J_{Ph}}{J_S}\right) - \ln\ln\left(\frac{J_{Ph}}{J_S}\right)\right] \quad (21)$$

The analytical peak power is finally expressed as:

$$P_{opt} = J_{opt} \times V_{opt} = \frac{J_{Ph}}{1 + \frac{1}{\ln\left(\frac{J_{Ph}}{J_S}\right)}} \times \frac{k\ T_m}{q}\left[\ln\left(\frac{J_{Ph}}{J_S}\right) - \ln\ln\left(\frac{J_{Ph}}{J_S}\right)\right] \quad (22)$$

3.2. Numerical Simulations

In this section, we substituted the Equation 15 in to the Equations (1), (3), (5), (6), (8), (9), and (14). The goal we are aiming here is to see analytically, how each electrical parameter is degraded during the module operating conditions, which allows us to estimate the degradation rate of each parameter as a function of the ambient temperature.

Given that, the ambient temperature is one of the most important factors that affects the module temperature, and therefore the global (PV)-cells/modules performance. Wind speeds used in our simulations, are the annual average of daily wind profiles of Cotonou measurement station at 10 m height from the ground.

3.3.1. Photocurrent Density (J_{ph})

Putting, the equation

$T_m = T_{amb} + d \times G(1 + e_0 \times T_{amb})(1 - f_o W)$ in to equation

$$J_{ph}(G,T) = J_{ph_{ref}}\left[1 + \alpha_{J_{SC}}\left(T_m - T_{ref}\right)\right] \frac{G}{G_{ref}},$$

we obtain:

$$J_{ph}(T_{amb}) = \frac{G J_{ph_{ref}}}{G_{ref}}\left[1 + \alpha_{J_{SC}}\left(T_{amb} + d \times G(1 + e_0 T_{amb})(1 - f_o W) - T_{ref}\right)\right]$$

$$J_{ph}(T_{amb}) = \frac{\alpha_{J_{SC}}.G.J_{ph_{ref}}}{G_{ref}}\left[\frac{1}{\alpha_{J_{SC}}} - T_{ref} + T_{amb} + d \times G(1 + e_0 \times T_{amb})(1 - f_o W)\right]$$

Variables declaration:

$$J_{phref} = 5.11 A/m^2 \; ; G_{ref} = 1 W/m^2 \; ; G = 1000 \; W/m^2$$

$$\alpha_{Jsc} = u = 7.5 \times 10^{-2} \; ; T_{ref} = 298 \text{ K}; d = 2.1 \times 10^{-2} \; °C.m^2/w \; ;$$

$$e_0 = 1.6 \times 10^{-2} \; °C^{-1} \; ; f_o = 7.5 \times 10^{-2}; W = 1.1 \times 10^{-3} \; m/S$$

We posed $t = \frac{u \times G \times J_{ph_{ref}}}{G_{ref}}$; $p = \frac{1}{u}$; $t_1 = p - T_{ref}$ and $S = d \times G \times (1 - f_o \times W)$

$$\text{Then } J_{ph}(T_{amb}) = t \times [t_1 + T_{amb} + S \times (1 + e_0 \times T_{amb})] \tag{23}$$

3.3.2. Series Resistance (R_S)

Putting, the equation $T_m = T_{amb} + d \times G(1 + e_0 \times T_{amb})(1 - f_o W)$ in to equation

$R_S(Tamb) = R_{S_{ref}} \times \frac{T_m}{T_{ref}}\left(1 - \beta \times ln\frac{G}{G_{ref}}\right)$, we have:

$$R_S(Tamb) = \frac{R_{S_{ref}}}{T_{ref}}(T_{amb} + d \times G(1 + e_0 \times T_{amb})(1 - f_o W))\left(1 - \beta \times ln\frac{G}{G_{ref}}\right)$$

Variables declaration:

$$Rs_{ref} = 5.11 \; \Omega \; ; T_{ref} = 298 \; K \; ; u = \beta = 4.5.10^{-1} \; ; G = 1000 \; W/m^2$$

$$d = 2.1 * 10^{-2} \; °C.m^2/w \; ; G_{ref} = 1w/m^2 \; ; e_0 = 1.6 \times 10^{-2} \; °C^{-1} \; ; f_o = 7.5 \times 10^{-2};$$

$W = 1.1 \times 10^{-3} \; m/S$. We posed $t_1 = \frac{R_{S_{ref}}}{T_{ref}}$; $V = \frac{G}{G_{ref}}$; $t_2 = (1 - u \times \ln(V))$: $t = t_1 \times t_2$ and

$S = d \times G \times (1 - f_o W)$, then:

$$R_S(Tamb) = \; t \times (T_{amb} + \; S \; \times (1 + e_0 \times T_{amb})) \tag{24}$$

3.3.3. PV Module Efficiency (η)

Substituting, the equation $T_m = T_{amb} + d \times G(1 + e_0 \times T_{amb})(1 - f_o W)$ in to equation

$$\eta = \; \eta_{T_{ref}}\left[1 - \beta_{ref}\left(T_m - T_{ref}\right) \; + \; \gamma \times logG_T\right]$$

we can write:

$$\eta = \; \eta_{T_{ref}}\left[1 + \; \gamma \times \log(G) + \beta_{ref} \times T_{ref} - \beta_{ref} \times (T_{amb} + d \times G(1 + e_0 \times T_{amb})(1 - f_o W))\right]$$

Variables declaration:

$$T_{ref} = 298 \; °K \; ; d = 2.110^{-2} C.m^2/w \; ;$$

$$e_0 = 1.6 \times 10^{-2}\ °C^{-1}; \beta_{ref} = V = 4.5 \times 10^{-3}\ ;$$

$$n_{ref} = 1.5 \times 10^{-1}\ \%\ ; \gamma = u = 5.3 \times 10^{-4}\ ;$$

$$G = 1000\ W/m^2$$

$$f_o = 7.5 \times 10^{-2}; W = 1.1 \times 10^{-3}\ m/S$$

We posed $t = 1 + u \times \log(G)$; $t_1 = V \times T_{ref}$;

$$t_2 = t + t_1\ ; S = d \times G \times (1 - f_o W)$$

$$\text{Then } \eta\ (Tamb) = \eta_{T_{ref}} \times [t_2 - V \times (T_{amb} + S \times (1 + e_0 \times T_{amb}))] \quad (25)$$

3.3.4. PV Module Power Output (P)

Putting, the equation $T_m = T_{amb} + d \times G(1 + e_0 \times T_{amb})(1 - f_o W)$ in to equation

$$P(Tamb) = G \times \tau_{pV} \times \eta_{ref} \times A \times \left[1 - V \times \left(T_m - T_{ref}\right)\right], \text{ we have:}$$

$$p(Tamb) = G_T \tau_{pV} \eta_{ref} A\left[1 + V \times T_{ref} - V \times (T_{amb} + d \times G \times (1 + e_0 \times T_{amb})(1 - f_o W))\right]$$

Variables declaration:

$$G = 1000\ W/m^2\ ; n_{ref} = 1.5.10^{-1}\ \%\ ;$$

$$\tau_{pV} = u = 3.8.10^{-1}; A = 4;$$

$$V = 4.5 \times 10^{-3}\ ; d = 2.1 \times 10^{-2} Cm^2/w\ ; T_{ref} = 298\ K\ ;$$

$$e_0 = 1.5 \times 10^{-2}\ °C^{-1}\ ; f_o = 7.5 \times 10^{-2}\ ;$$

$$W = 1.1 \times 10^{-3}\ m/S$$

We posed $p_1 = A \times G \times u \times \eta_{ref}$; $t = 1 + V \times T_{ref}$ and $S = d \times G \times (1 - f_o W)$

$$\text{Then } p(Tamb) = p_1 \times [t - V \times (T_{amb} + S \times (1 + e_0 \times T_{amb}))] \quad (26)$$

3.3.5. Shunt Resistance (R_{Sh})

Substituting, the equation $T_m = T_{amb} + d \times G(1 + e_0 \times T_{amb})(1 - f_o W)$ in to equation

$$R_{Sh} = R_{Sho} - m_o \times T_m,$$

we have :

$$R_{Sh}(Tamb) = R_{Sho} - m_o \times [T_{amb} + d.G(1 + e_0 T_{amb})(1 - f_o W)]$$

$$R_{Sh}(Tamb) = m_o \times [\frac{R_{Sho}}{m_o} - T_{amb} - d \times G \times (1 + e_0 \times T_{amb})(1 - f_o W)]$$

Variables declaration:

$$m_o = 6.8936\ \Omega Cm^2/K; R_{Sho} = 3858.86\ \Omega Cm^2/K;$$

$$d = 2.1 \times 10^{-2} C.m^2/w\ ;$$

$$G = 1000\ W/m^2\ ; f_o = 7.5 \times 10^{-2}\ ;$$

$$e_0 = 1.6 \times 10^{-2}\ °C^{-1}\ ;$$

$W = 1.1 \times 10^{-3}\ m/S$. We posed $u = \frac{R_{Sho}}{m_o}$ and

$$S = d \times G \times (1 - f_o W)$$

Then

$$R_{Sh}(Tamb) = m_o \times [u - T_{amb} - S \times (1 + e_0 \times T_{amb})] \quad (27)$$

3.3.6. Open-Circuit Voltage (V_{OC})

Putting, the equation

$T_m = T_{amb} + d \times G(1 + e_0 \times T_{amb})(1 - f_o W)$ in to equation

$$V_{OC}(Tamb) = \frac{E_g}{q} - \frac{nkT_m}{q} \times \ln\left(\frac{J_S}{J_{ph}}\right),$$

we have:

$$V_{OC}(Tamb) = \frac{E_g}{q} - \frac{nk}{q}(T_{amb} + d \times G \times (1 + e_0 \times T_{amb})(1 - f_o W)) \times \log\left(\frac{J_S}{J_{ph}}\right)$$

Variables declaration:

$$Eg = 1.884 \times 10^{-19}\ \text{J}\ ;\ n = 1.25\ ;\ q = 1.6.10^{-19} C\ ;\ J_{ph} = 5.11\ A/m^2\ ;\ J_s = 0.9\ A/m^2\ ;\ G = 1000\ W/m^2\ ;$$

$$k = 1.38 \times 10^{-23}\ ;\ d = 2.1 \times 10^{-2} C.m^2/w\ ;\ e_0 = 1.5 \times 10^{-2}\ °C^{-1}\ ;$$

$$f_o = 7.5 \times 10^{-2}\ ;\ W = 1.1 \times 10^{-3}\ m/S.$$

We posed $= \frac{n \times k}{q}$; $u = \frac{J_S}{J_{ph}}$; $p = \log(u)$; $t_1 = \frac{E_g}{q}$; $S = d \times G \times (1 - f_o \times W)$; $t_3 = p \times t$ and $t_4 = \frac{t_1}{t_3}$

$$\text{Then, } V_{OC}(Tamb) = t_3 \times (t_4 - T_{amb} - S \times (1 + e_0 \times T_{amb})) \quad (28)$$

3.3.7. Saturation Current Density (J_S)

Substituting, the equation $T_m = T_{amb} + d \times G \times (1 + e_0 \times T_{amb})(1 - f_o W)$ in to equation

$$J_S = J_{S_{ref}} \times \left(\frac{T_m}{T_{ref}}\right)^{\frac{3}{n}} \times exp\left(\left(\frac{E_g(T)}{n \times K}\right)\left(\frac{1}{T_{ref}} - \frac{1}{T_m}\right)\right),$$

we obtain:

$$J_S = J_{S_{ref}} \times \left(\frac{T_{amb} + d \times G \times (1 + e_0 \times T_{amb})(1 - f_o W)}{T_{ref}}\right)^{\frac{3}{n}} \times exp\left(\left(\frac{E_g(T)}{n \times K}\right)\left(\frac{1}{T_{ref}} - \frac{1}{T_{amb} + d \times G \times (1 + e_0 \times T_{amb})(1 - f_o W)}\right)\right)$$

Variables declaration:

$$Js_{ref} = 1.2.10^{-3} A/m^2\ ;\ T_{ref} = 298\ °K\ ;\ d = 2.1 \times 10^{-2} °C \times m^2/w\ ;$$

$$G = 1000 W/m^2;\ e_0 = 1.5 \times 10^{-2}\ °C^{-1}\ ;\ f_o = 7.5 \times 10^{-2};$$

$$W = 1.1 \times 10^{-3}\ m/S\ ;\ n = 1.25\ ;\ E_g(T) = 1.884 \times 10^{-19}\ \text{Joule}\ ;$$

$k = 1.38 \times 10^{-23}$. We posed $u = \frac{3}{n}$; $t = \frac{E_g(T)}{n \times k}$; $t_1 = \frac{1}{T_{ref}}$; $s = d \times G$;

$$z = 1 - f_o \times W\ ;\ t_2 = s \times z \text{ and } t_3 = t_1 \times t_2$$

$$\text{Then } J_S(T_{amb}) = J_{S_{ref}} \times \left(t_1 \times T_{amb} + t_3 \times (1 + e_0 \times T_{amb})\right)^u \times exp\left(t \times \left(t_1 - \frac{1}{T_{amb} + t_2 \times (1 + e_0 \times T_{amb})}\right)\right) \quad (29)$$

3.4. Results Interpretation

We revealed that solar cells/modules degradation is strongly caused by three important factors resulting in a gradual degradation in module performance. These factors are: (i) an increase in the cell's series resistance (R_S), (ii) a decrease in the cell's shunt resistance (R_{Sh}), (iii) and an anti-reflection coating deterioration. (Figure 1) shows the one-diode equivalent-circuit model of the solar cell used, illustrating the series (R_S) and shunt (R_{Sh}) resistances. These cell specific degradation modes are important factors in analyzing PV cell/module degradation and failures. In this study, the dependence of performance parameters (J_{Ph}), (R_S), (V_{OC}), (R_{Sh}), (P), (η) and (J_S) under the illumination

intensity of 1000 W/m^2 at different temperatures is shown from (figure 2) to (figure 8). The parameters (V_{OC}) (figure 2), (R_{Sh}) (figure 3), and (η) (figure 4), decrease linearly with T while (R_S) (figure 5) increase linearly with ambient temperature. In addition, (J_{Ph}) (figure 6) and (J_S) (figure 7) increase exponentially with temperature, while the obtained power output (P) (figure 8) decrease exponentially. The decrease in power output (P) of the crystalline silicon modules has been found to be mainly due to degradation in the short-circuit current density (J_{SC}), and to a lesser extent, the fill factor (FF). The likely cause for reduction in short-circuits current density (J_{SC}) is the physical degradation of the encapsulant (like discoloration and delamination), and for the reduction in fill factor (FF) it's increases in series resistance (R_S) due to corrosion [48].

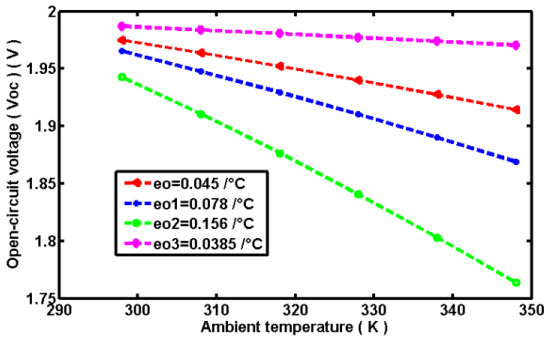

Figure 2. *Normalized plot of open-circuit voltage (V_{OC}) with temperature in the range 298-348 K. This curve is analytically obtained from Equation (28) as a function of the ambient temperature.*

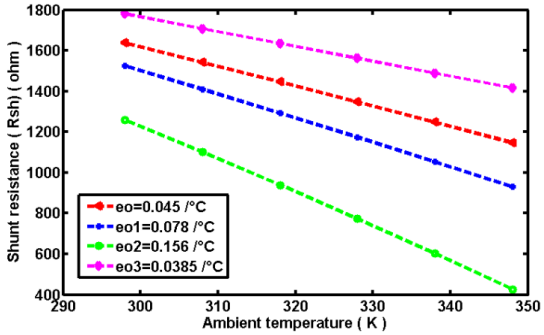

Figure 3. *Normalized plot of shunt resistance (R_{Sh}) with temperature in the range 298-348 K. This curve is analytically obtained from Equation (27) as a function of the ambient temperature.*

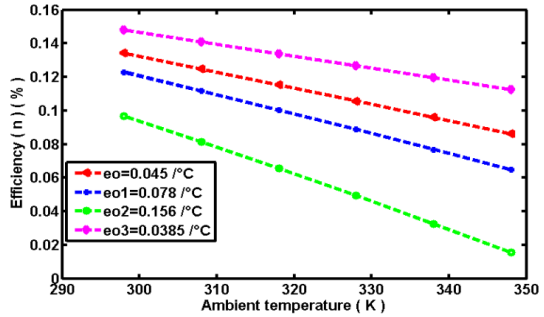

Figure 4. *Normalized plot of Efficiency (η) with temperature in the range 298-348 K. This curve is analytically obtained from Equation (25) as a function of the ambient temperature.*

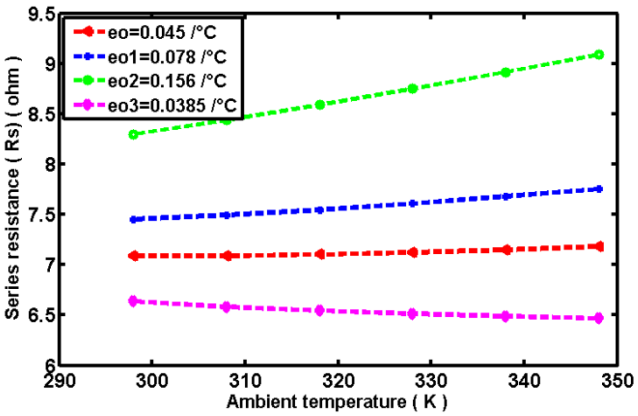

Figure 5. *Normalized plot of series resistance (R_S) with temperature in the range 298-348 K. This curve is analytically obtained from Equation (24) as a function of the ambient temperature.*

According to [48], low shunt resistance (R_{Sh}) detracts significantly from the cell/module performance. Ideally, should be infinitely large. This parameter is crucial to PV performance, especially at reduced irradiance levels. We noted a significant correlation between the degradation of power output (P) and (FF). This coefficient is about 0.86, which indicates that the reduction of (P) is mainly due to the decrease of (FF).

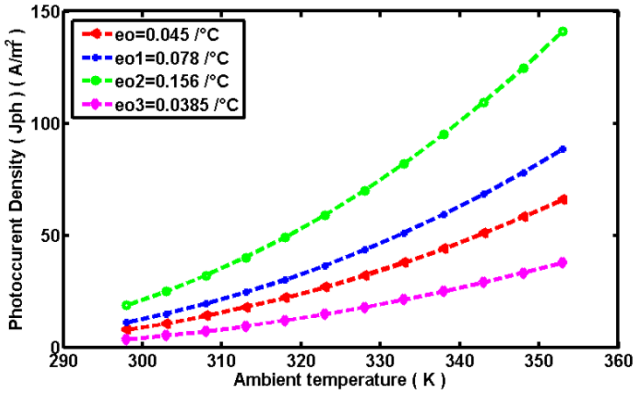

Figure 6. *Normalized plot of photocurrent density (J_{ph}) with temperature in the range 298-348 K. This curve is analytically obtained from Equation (23) as a function of the ambient temperature.*

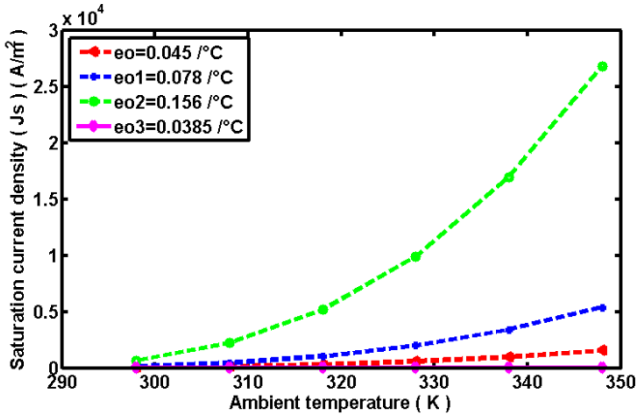

Figure 7. *Normalized plot of Saturation current density (J_S) with temperature in the range 298-348 K. This curve is analytically obtained from Equation (29) as a function of the ambient temperature.*

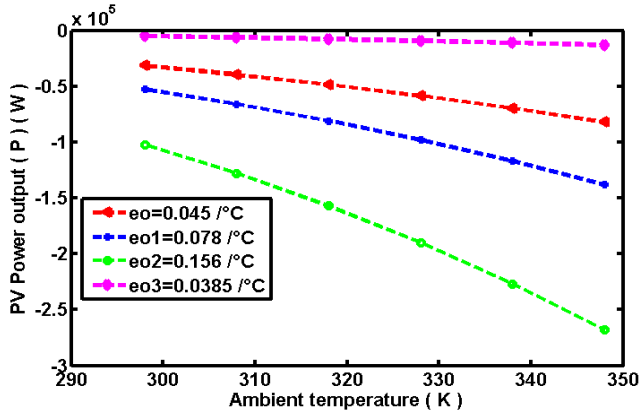

Figure 8. *Variation of PV module output (P) with temperature in the range 295-348 K. This curve is analytically obtained from Equation (26) as a function of the ambient temperature.*

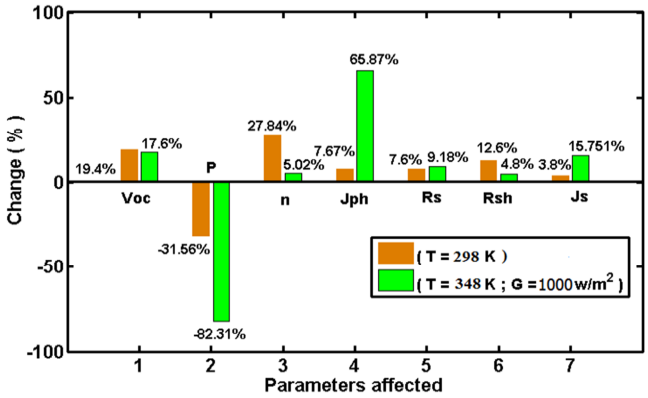

Figure 9. *Changes in the analytically obtained PV cell/module parameters for an increase in temperature between 298 K and 348 K, under standard irradiation conditions (STC) (G=1000W/m^2).*

The relative changes (in percentage) of the seven (PV)-cell/module parameters (V_{OC}; P; η; J_{Ph}; R_S; R_{Sh} and J_S) are illustrated in (figure 9). As shown in figure 9, statistical data describe very well the empirical data represented by the functions ($J_{Ph}(T_{amb})$; $R_S(T_{amb})$; $p(T_{amb})$; $\eta(T_{amb})$; $R_{Sh}(T_{amb})$; $V_{OC}(T_{amb})$ and $J_S(T_{amb})$). Statistical data shown as red wine rectangle, indicate the degradation of each parameter at 298 K, while green rectangle shows the relative changes, in percentage at 348 K.

Globally, (J_{Ph}) increases strongly (7.67% to 65.87%) when T increases from 298 K to 353 K. We note a small increase in saturation current density (J_S) by 3.8% and 15.76% with temperature (figure 9), which can be attributed to the increased light absorption owing to a decrease in the bandgap of silicon. The decrease of (η) (27.84% to 5.02%) (figure 9) with temperature is mainly controlled by the decrease of (V_{OC}) (19.4% to 17.6%) and fill factor (FF) with T (figure 9). It can be seen that with the temperature increasing, the (J_{SC}) increases slightly and the (V_{OC}) decreases strongly. The slight increase of (J_S) in this study, similar to the effects of (J_{SC}) originates from the narrowing of the band gap along with the increase in the number of phonons and density of states in the conduction and valence bands, while the strong decrease in the (V_{OC}) is mainly linked to the increase of the leakage current [60], owing to the decrease of (R_{Sh}) (12.6% to 4.8%) (figure 9). As a result, the maximum output power decreases with the temperature increasing. For a standard solar cell, the (J_{SC}) can be strongly influenced by the minority carrier diffusion length which depends on the product of the minority electron mobility and carrier lifetime. In addition, the decrease rate of (V_{OC}) is about 19.40% and is much larger in magnitude than decrease of Rs with T. The rate of decrease in the maximum output power (P) is 31.56% while that of the efficiency (η) is about 12.82%. This result is very significant in our work because, the effect of heat and irradiance are the factors that negatively affect the overall performance of (PV)-cells. The increase in series resistance (R_S) (7.6% to 9.18%) (figure 9) has been identified as the prominent reason for module performance degradation. This result has been obtained and validated by several works.

3.5. Comparison

Here, to validate our model, we calculated the Percentage degradation rates of maximum output power (P_{max}), short-circuit current (I_{SC}), open circuit voltage (V_{OC}) and fill factor (FF). Ours theoretical results obtained have been compared with those obtained by [61]. We determined the degradation rate using the expression [3]:

$$RD(\%) = (1 - \frac{VP_{deg}}{VP_{in}}) \times 100 \qquad (30)$$

Where VP_{deg} represents the parameter value after degradation and VP_{in} the initial value of the considered parameter (P_{max}; I_{SC}; V_{OC} and FF).

Table 3 summarizes the comparison of the different degradation rates obtained.

Table 3. *Comparison of the different degradation rates obtained.*

Technology type	Parameters	Initial value (Reference)	Global degradation	Degradation rate (%/)
Poly-c-Si PWX500 [71]	P_{max} (W)	50	31.56	36.88
	V_{OC} (V)	21.6	19.64	09.05
	I_{SC} (A)	3.18	3.023	04.94
	FF (%)	72	62.64	13.41
Poly-c-Si BPS150 This study	P_{max} (W)	150	102.66	31.56
	V_{OC} (V)	21.60	17.41	19.40
	I_{SC} (A)	09.08	08.73	3.8
	FF (%)	72	67.38	6.42

The degradation rate is used to evaluate the long-term changes in the performance of (PV)-modules. It provides

important information about the overall effect of losses. From Table 3 we noticed that the degradation rate differs from one module to another.

In addition, the degradation rate is higher in open circuit voltage (Voc) for the module (Poly-c-Si BPS150) while Fill factor (FF) is more degraded with module Poly-c-Si PWX500.

From Table 3, evaluation of performance parameters of polycrystalline silicon modules (PWX-500) and (Poly-c-Si BPS150) showed the high effect of heat stress on the efficiency and performance of this technology with time. Power losses analysis shows that these modules do not have reliability in tropical environments and do not respect guaranty conditions.

4. Conclusions

The behaviour of BPS150-36 Polycrystalline electrical Parameters with Ambient Temperature under standard irradiation conditions (G=1000 W/m^2) in the 298-348K temperature range has been investigated analytically, using the Servant model. The transcendental single exponential model has been used to extract the (PV)-cell parameters from a single (*J-V*) characteristic curve at various values of T. MATLAB software with r.getdata has been exploited to perform the numerical simulations.

Simulated results show that (J_{Ph}) increases exponentially from 7.67% to 65.87% with temperature. (R_S) increases linearly by 7.6% and 9.18% while (V_{OC}) decreases from 19.4 % to 17.6% and (R_{Sh}) decreases approximately by 12.6% and 4.8%. The power output (P) losses decreases by 82.31 % and 31.56%, and the overall linear losses in efficiency (η) has been approximately 27.84% and 5.02%, while (J_S) increase exponentially from 3.87% to 15.75%.

In definitive, the increase in (J_{ph}) with temperature can be attributed to the increased in light absorption owing to a decrease in the bandgap of silicon. The decrease in (η) with temperature is mainly controlled by the decrease in (V_{OC}) and fill factor (FF) with T. The increase in (Rs) is affected by the variation of temperature, leading to the loss of power (P) and Fill Factor (FF). The decrease in (Voc) with T, indicates the existence of high parasitic series resistance, and mainly linked to the increase of the leakage current. As a result, the maximum output power decreases with the temperature increasing. This loss is due to decrease of (J_{SC}) and (Voc) with the temperature increasing that lead to reduce the (PV)-modules optical properties. Elevated temperatures can drastically change the mechanical, electrical, and optical properties of polymeric materials, as a result, a drop of the PV cells/modules overall efficiency.

Future work can be about:

(1) Compare experimental results obtained by Mattei model with those obtained analytically,

(2) Compare analytically Servant model with Mattei model.

References

[1] Schneller E J., Brooker R P., Shiradkar N S., Dhere N G., Davis K O., Seigneur H P., Mohajeri N., Wohlgemuth J., Scardera G., Rudack A C., Schoenfeld W V. (2016): Manufacturing metrology for c-Si module reliability and durability Part III: Module manufacturing. Renewable and Sustainable Energy Reviews, 59: 992-1016.

[2] Parretta A., Bombace M., Graditi G., Schioppo R. (2005): Optical degradation of long-term, field-aged c-Si photovoltaic modules. Solar Energy Materials and Solar Cells, 86: 349-364.

[3] Kahoul N., Houabes M., Sadok M. (2014): Assessing the early degradation of photovoltaic modules performance in the Saharan region. Energy Conversion and Management, 82: 320-326.

[4] Munoz M A., Alonso-Garcı M C., Vela N., Chenlo F. (2011): Early degradation of silicon PV modules and guaranty conditions. Solar Energy, 85: 2264-2274.

[5] Ketola B., Shirk C., Griffith P. (2011): Encapsulation performance comparison of PV modules in outdoor arrays. In Proceedings of the 26th European Photovoltaic Solar Energy Conference and Exhibition, 3144-3151.

[6] Sharma V., Chandel S S. (2013): Performance and degradation analysis for long term reliability of solar photovoltaic systems: A review. Renewable Sustainable Energy Reviews, 27: 753-767.

[7] Dubey R., Chattopadhyayl S., Kuthanazhil V., Johnl J J., Vasil J., Kottantharayill A., Arora B M., Narsimhanl K L., Kuber V., Solanki C S., Kumar A., Sastry O S. (2014): Performance degradation in field-aged crystalline silicon PV modules in different Indian climatic conditions. In Proceedings of the IEEE 40th Photovoltaic Specialists Conference, 3182-3187.

[8] Kichou S., Santiago S., Gustavo N., Torres R M., Chouder A., Guasch D. (2016): Characterization of degradation and evaluation of model parameters of amorphous silicon photovoltaic modules under outdoor long-term exposure. Energy, 96: 231-241.

[9] Park N C., Jeong J S., Kang B J., Kim D H. (2013): The effect of encapsulant discoloration and delamination on the electrical characteristics of photovoltaic module. Microelectronics Reliability, 53: 1818-1822.

[10] Tossa A K., Soro Y M., Thiaw L., Azoumah Y., Sicot L., Yamegueu D., Lishou C., Coulibaly Y., Razongles G. (2016): Energy performance of different silicon photovoltaic technologies under hot and harsh climate. Energy, 103: 261-270.

[11] Canete C., Carretero J., Cardona S M. (2014): Energy performance of different photovoltaic module technologies under outdoor conditions. Energy, 65: 295-302.

[12] Makrides G., Zinsser B., Georghiou G E., Schubert M., Werner J H. (2009): Temperature behaviour of different photovoltaic systems installed in Cyprus and Germany. Solar Energy Materials and Solar Cells, 93: 1095-9.

[13] Amrouche B., Sicot L., Guessoum A., Belhamel M. (2013): Experimental analysis of the maximum power point's properties for four photovoltaic modules from different technologies: monocrystalline and polycrystalline silicon, CIS and CdTe. Solar Energy Materials and Solar Cells, 118: 124-34.

[14] Khan F., Singh S N., Husain M. (2010): Effect of illumination intensity on cell parameters of a silicon solar cell. Solar Energy Materials and Solar Cells, 94: 1473-6.

[15] Singh P., Ravindra N M. (2012): Temperature dependence of solar cell performance-ananalysis. Solar Energy Mater Sol Cells, 101: 36-45.

[16] Meral M E., Dincer F. (2011): A review of the factors affecting operation and efficiency of photovoltaic based electricity generation systems. Renewable and Sustainable Energy Reviews, 15: 2176-84.

[17] Sanchez Reinoso C R., Milone D H., Buitrago R H. (2010): Efficiency study of different photovoltaic plant connection schemes under dynamic shading. International Journal of Hydrogen Energy, 35: 5838-43.

[18] Nagae S, Toda M, Minemoto T, Takakura H, Hamakawa Y. (2006): Evaluation of the impact of solar spectrum and temperature variations on output power of silicon-based photovoltaic modules. Solar Energy Materials and Solar Cells, 90: 3568-75.

[19] Park K., Kang G., Kim H., Yu G., Kim J. (2010): Analysis of thermal and electrical performance of semi-transparent photovoltaic (PV) module. Energy, 35: 2681-7.

[20] Géraud F H., Basile B K., Macaire A., Irénée V M. (2018): Degradation of Crystalline Silicon Photovoltaic Cells/Modules under Heat and Temperature Effect. Physical Science International Journal, 19: 1-12.

[21] Sanchez-Friera P., Piliougine M., Peläez J., Carretero J., Cardona M S. (2011): Analysis of degradation mechanisms of crystalline silicon PV modules after 12 years of operation in Southern Europe. Progress in Photovoltaics Research and Application, 19: 658-666.

[22] Joseph M K., Rong P., Tamizhmani G S. (2014): Investigation of dominant failure mode (s) for field-aged crystalline silicon PV modules under desert climatic conditions. IEEE Journal of Photovoltaics, 4: 814-826.

[23] Sharma V., Kumar A., Sastry O S., Chandel S S. (2011): Performance assessment of different solar photovoltaic technologies under similar outdoor conditions. Energy, 58: 511-551.

[24] Alshushan M A., Saleh I M. (2013): Power degradation and performance evaluation of PV modules after 31 years of work. IEEE 39th Photovoltaic Specialists Conference, 2977-2982.

[25] Pramod R., Tiwari G N., Sastry O S., Birinchi B., Vikrant S. (2016): Degradation of monocrystalline photovoltaic modules after 22 years of outdoor exposure in the composite climate of India. Solar Energy, 135: 786-795.

[26] Huili H., Xian D., Haiwen L., Huan Y., Kai Z., Jiangfeng L., Verlinden P J., Zongcun L., Hui S. (2018): Analysis of the Degradation of Monocrystalline Silicon Photovoltaic Modules After Long-Term Exposure for 18 Years in a Hot-Humid Climate in China. IEEE Journal of Photovoltaics, 8: 806-812.

[27] Dunlop E D., Halton D. (2006): The performance of crystalline silicon photovoltaic solar modules after 22 years of continuous outdoor exposure. Progress in Photovoltaics Reseach and Applications, 14: 53-64.

[28] Sakamoto S., Oshiro T. (2003): Field test results on the stability of crystalline silicon photovoltaic modules manufactured in the 1990's. In 3rd World Conference on Photovoltaic Energy Conversion, Osaka, Japan, 1888-1891.

[29] Sastry O S., Saurabh S., Shil S K., Pant P C., Kumar R., Bandyopadhyay B. (2010): Performance analysis of field exposed single crystalline silicon modules. Solar Energy Materials and Solar Cells, 94: 1463-1468.

[30] Jordan D C., Kurtz S R. (2013): Photovoltaic degradation rates-an analytical review. Progress in Photovoltaics Research and Application, 21: 12-29.

[31] Chandel S S., Naik M N., Sharma V., Chandel R. (2015): Degradation analysis of 28-year field exposed mono-c-Si photovoltaic modules of a direct coupled solar water pumping system in western Himalayan region of India. Renewable Energy, 78: 193-202.

[32] Ndiaye A., Kebe C M F., Charki A., Ndiaye P A., Sambou V., Kobi A. (2014): Degradation evaluation of crystalline-silicon photovoltaic modules after a few operation years in a tropical environment. Solar Energy, 103: 70-77.

[33] Bouraiou A., Hamouda M., Chaker A., Mostefaoui M., Lachtar S., Sadok M., Boutasseta N., Othmani M., Issam A. (2015): Analysis and evaluation of the impact of climatic conditions on the photovoltaic modules performance in the desert environment. Energy Conversion and Management, 106: 1345-1355.

[34] Ndiaye A., Kobi A., Charki A., Sambou V. (2013): Degradations of silicon photovoltaic modules: A literature review. Solar Energy, 96: 140-151.

[35] Servant J. (1976): Calculation of cell temperature for photovoltaic modules from climatic data, Proceedings of the 9th Biennial Congress of the International Solar Energy Society- Intersol, Montreal, Canada, 3: 1640-1643.

[36] Rouholamini A., Pourgharibshahi H., Fadaeinedjad R., Abdolzadeh M. (2014): Temperature of a photovoltaic module under the influence of different environmental conditions-experimental investigation. International Journal of Ambient Energy, 37: 266-272.

[37] Radziemska E. (2003): The effect of temperature on the power drop in crystalline silicon solar cells. Renewable Energy, 28: 1-12.

[38] Siddiqui M U., Abido M. (2013): Parameter estimation for five and seven-parameter photovoltaic electrical models using evolutionary algorithms. Applied Softward Computing, 13: 4608-4621.

[39] Ma T., Yang H., Lu L. (2014): Development of a model to simulate the performance characteristics of crystalline silicon photovoltaic modules/strings/arrays. Solar Energy, 100: 31-41.

[40] Bai J., Liu S., Hao Y., Zhang Z., Jiang M., Zhang Y. (2014): Development of a new compound method to extract the five parameters of PV modules. Energy Conversion and Management, 79: 294-303.

[41] Attivissimo F., Adamo F., Carullo A., Lanzolla A M L., Spertino F., Vallan A. (2013): On the performance of the double-diode model in estimating the maximum power point for different photovoltaic technologies. Measurement, 46: 3549-3559.

[42] Ishaque K., Salam Z., Syafaruddin A. (2011): Comprehensive MATLAB Simulink PV system simulator with partial shading capability based on two-diode model. Solar Energy, 85: 2217-2227.

[43] Ishaque K., Salam Z., Taheri H. (2011): Simple, fast and accurate two-diode model for photovoltaic modules. Solar Energy Materials and Solar Cells, 95: 586-594.

[44] Tossa A K., Soro Y M., Azoumah Y., Yamegueu D. (2014): A new approach to estimate the performance and energy productivity of photovoltaic modules in real operating conditions. Solar Energy, 110: 543-560.

[45] Ghani F., Duke M., Carson J. (2013): Numerical calculation of series and shunt resistance of a photovoltaic cell using the Lambert W-function: experimental evaluation. Solar Energy, 87: 246-253.

[46] Ghani F., Duke M. (2011): Numerical determination of parasitic resistances of a solar cell using the Lambert W-function. Solar Energy, 85: 2386-2394.

[47] Alami A H. (2014): Effects of evaporative cooling on efficiency of photovoltaic modules. Energy Conversion Management, 77: 668-79.

[48] Meyer E L., van Dyk E E. (2004): Assessing the reliability and degradation of photovoltaic module performance parameters. IEEE Transactions on Reliability, 53: 83-92.

[49] Daliento S., Lancellotti L. (2010): 3D analysis of the performances degradation caused by series resistance in concentrator solar cells. Solar Energy, 84: 44-50.

[50] Alonso G M C., Balenzategui J L. (2004): Estimation of photovoltaic module yearly temperature and performance based on Nominal Operation Cell Temperature calculations. Renewable Energy, 29: 1997-2010.

[51] Skoplaki E., Palyvos, J A. (2009): On the temperature dependence of photovoltaic module electrical performance: A review of efficiency/power correlations. Solar Energy, 83: 614-624.

[52] Zondag H A. (2008): Flat-plate PV-thermal collectors and systems - a review. Renewable and Sustainable Energy Reviews, 12: 891-959.

[53] Garg H P., Agarwal R K. (1995): Some aspects of a PV/T collector/forced circulation flat plate solar water heater with solar cells. Energy Conversion and Management, 36: 87-99.

[54] Evans D L., Florschuetz L W. (1978): Terrestrial concentrating photovoltaic power system studies. Solar Energy, 20: 37-43.

[55] Evans D L. (1981): Simplified method for predicting photovoltaic array output. Solar Energy, 27: 555-560.

[56] Kou Q., Klein S A., Beckman W A. (1998): A method for estimating the long-term performance of direct-coupled PV pumping systems. Solar Energy, 64: 33-40.

[57] Siegel M D., Klein S A., Beckman W A. (1981): A simplified method for estimating the monthly-average performance of photovoltaic systems. Solar Energy, 26: 413-418.

[58] Jie J., Hua Y., Gang P., Bin J., Wei H. (2007): Study of PV-Trombe wall assisted with DC fan. Building and Environment, 42: 3529-3539.

[59] Evdokimov V M., Maiorov V A. (2017): A Study of Limiting Energy and Temperature Characteristics of Photovoltaic Solar Radiation Converters. Applied Solar Energy, 53: 1-9.

[60] Chengquan X., Xuegong Y., Deren Y., Duanlin Q. (2014): Impact of solar irradiance intensity and temperature on the performance of compensated crystalline silicon solar cells. Solar Energy Materials and Solar Cells, 128: 427-434.

[61] Kahoul N., Chenni R., Cheghib H., Mekhilef S. (2017): Evaluating the reliability of crystalline silicon photovoltaic modules in harsh environment. Renewable Energy, 109: 66-72.